

The Knowable Future: Mapping the Decay of Past–Future Mutual Information Across Forecast Horizons

Peter Maurice Catt

*School of Computing, Electrical and Applied Technology
UNITEC Institute of Technology, Auckland, New Zealand*

Abstract

Forecasting fails not because models are weak, but because effort is wasted on series whose futures are fundamentally unknowable. We propose a pre-modelling diagnostic framework that assesses horizon-specific forecastability before model selection begins, enabling practitioners to allocate effort where it can yield returns.

We operationalise forecastability as auto-mutual information (AMI) at lag h , measuring the reduction in uncertainty about future values provided by the past. Using a k-nearest-neighbour estimator on training data only, we validate AMI against realised out-of-sample error (sMAPE) across 1,350 M4 series spanning six frequencies, with Seasonal Naïve, ETS, and N-BEATS as probe models under a rolling-origin protocol.

The central finding is that the AMI–sMAPE relationship is strongly frequency-conditional. For Weekly, Hourly, Quarterly, and Yearly series, AMI exhibits consistent negative rank association with realised error (Spearman ρ ranging from -0.52 to -0.66 for higher-capacity probes), supporting its use as a triage signal. Monthly shows moderate association; Daily exhibits weaker discrimination despite measurable dependence. Across all frequencies, median forecast error decreases monotonically from low to high AMI terciles, confirming decision-relevant separation.

These results establish AMI as a practical screening tool for forecasting portfolios: identifying series where sophisticated modelling is warranted, where baselines suffice, and where effort should shift from accuracy improvement to robust decision design.

Keywords: Forecastability; predictive information; mutual information; time series; M4 competition; decision analytics; forecast error; forecasting

1. Introduction

Forecasting portfolios rarely fail because models are weak; they fail because effort is applied indiscriminately to series whose futures contain little usable information. Some series respond well to sophisticated methods. Others show no improvement over simple baselines, regardless of model complexity or computational investment (Makridakis et al., 2018). The practical question is: which series justify sophisticated modelling effort, and which do not?

Current practices rely on trial and error. Practitioners build models, evaluate performance, then refine or abandon approaches based on results. This is operationally inefficient. If a series lacks exploitable structure at relevant horizons, model tuning is unlikely to improve forecasts substantially. Time and resources should be allocated elsewhere or focused on mitigating forecast error impacts rather than reducing errors that cannot be reduced (Kolassa, 2009).

Forecastability assessment should happen before model building begins. The question is whether a series contains predictive information at horizons that matter for decisions. This is a property of the time series itself (given a declared information set), not a property of a particular forecasting model. A series with strong organised patterns is forecastable even if current models perform poorly. Conversely, a series with weak temporal structure is difficult to forecast regardless of method sophistication.

We estimate horizon-specific forecastability and validate it against realised accuracy; we do not claim a universal ‘forecast horizon’ boundary. The goal is operational triage, not theoretical characterisation of forecastability limits.

Classical variability measures like standard deviation or coefficient of variation do not address this. A volatile series with large seasonal swings can be easier to forecast than a smooth series drifting randomly. What matters is not how much a series varies, but how much the past tells us about the future (Catt, 2009). High variability with strong patterns is forecastable. Low variability with random drift is not.

The challenge is making forecastability operational. We need a measure that can be computed from historical data alone, estimated before forecasting begins, and validated against actual out-of-sample performance. It must handle heterogeneous series lengths and acknowledge that forecastability varies by horizon. A single score ignoring horizon is meaningless (Tiao & Tsay, 1994).

This paper adopts an information-theoretic view of forecastability as measurable past–future dependence (Bialek et al., 2001; Jaynes, 1957). We define forecastability at horizon h as mutual information $I(\text{Past}; \text{Future}_h)$, the reduction in uncertainty about the future obtained by observing the past. High mutual information indicates organised, exploitable structure. Low mutual information indicates weak or unexploitable dependence between past and future observations. We make no assumptions about the underlying data-generating process, which may be latent and time-varying, and instead focus on measurable past–future dependence in the realised data. AMI therefore quantifies an observable consequence of the data-generating mechanism—namely, how much predictive information persists at a given horizon without requiring parametric, structural, or stationarity assumptions about its form.

AMI is interpreted ordinally (rank-based), not metrically; our conclusions depend on whether AMI correctly orders series by forecastability, not on absolute mutual information values or estimator-specific units.

Contributions. This study makes two primary contributions:

1. A pre-modelling triage framework for allocating modelling effort by series and horizon. We provide a practical method for classifying series into action categories (invest in modelling / model cautiously / manage uncertainty) based on ex-ante forecastability assessment. This is the primary contribution for decision support.
2. Empirical validation. We demonstrate that AMI computed from training data correlates with out-of-sample forecast error (sMAPE) in frequency-dependent patterns, validating AMI as a pre-modelling diagnostic. Three probe models (Seasonal Naïve, ETS, N-BEATS) spanning different representational capacities confirm that the relationship holds across model classes, though strength and direction vary.

The methodology is tested on M4 competition series across six frequencies (Makridakis et al., 2020). The goal is not competition performance but decision analytics. The question is not ‘Can we beat benchmark X?’ but ‘Which series justify investment in methods beyond benchmark X?’ This reframes forecasting from a universal accuracy contest to a portfolio optimisation problem. The diagnostic answers not ‘which model is best?’ but ‘is this series worth modelling at all?’

We test AMI as a pre-modelling diagnostic under a fixed-information protocol with rolling-origin evaluation (10 origins per series). Diagnostics are computed strictly pre-origin from training data only, while forecast errors are evaluated post-origin and then averaged across origins to reduce single-origin variance. Observed associations are empirical and frequency-conditional rather than universal laws of predictability. Conceptually, we separate *forecastability* (available past–future dependence) from *exploitability* (model-specific ability to convert that dependence into lower loss).

The remainder of the paper is organised as follows: Section 2 reviews related work, Section 3 describes the experimental protocol, Section 4 presents the data and models, Section 5 reports the empirical results, Section 6 discusses implications and limitations, and Section 7 concludes.

2. Conceptual Foundations

2.1 The Forecastability Problem

Forecasting competitions from M1 onwards show that simple methods remain competitive on average (Makridakis et al., 1982; Makridakis & Hibon, 2000; Petropoulos et al., 2022). This is sometimes misinterpreted as ‘sophistication doesn’t help’. The correct interpretation is that average forecastability across competition portfolios is moderate. Sophisticated methods excel on high-signal series but struggle on low-signal series where they overfit noise. Simple methods perform adequately on low-signal series but underperform on high-signal series. The average difference narrows.

This supports rather than contradicts the forecastability thesis. Different series have fundamentally different information content. Method selection should respect this. Applying sophisticated methods to all series wastes resources on those that cannot benefit.

2.2 Existing Approaches and Their Limitations

The forecastability problem has been addressed through statistical, information-theoretic, model-based, and practical approaches, each with distinct strengths and limitations.

Statistical measures. The coefficient of variation ($CV = \sigma/\mu$) is widely used in practice to assess forecast difficulty (Gilliland, 2010), but CV conflates signal and noise. A series with large seasonal swings (high CV) may be easier to forecast than one with small random drift (low CV). Classical measures like autocorrelation functions and spectral decomposition identify structure but do not aggregate information into horizon-specific forecastability scores.

Information-theoretic and spectral approaches. Entropy-based measures quantify regularity and pattern complexity (Pincus 1991). Sample entropy (Richman & Moorman, 2000) measures the likelihood that similar patterns persist, with lower entropy indicating higher predictability. Catt (2014) demonstrated that sample entropy provides useful ex-ante indication of forecast accuracy on M3 data, though subject to limitations with intermittent demand and structural breaks. Goerg (2013) introduced Forecastable component analysis (ForeCA), defining forecastability via spectral entropy, with lower spectral entropy indicating higher forecastability. These measures capture pattern complexity that CV cannot, but they produce single global scores that do not vary by horizon.

Model-based and dynamical systems approaches. In econometrics, predictability is measured through variance decomposition or predictive R^2 (Stock & Watson, 2003). Lyapunov exponents quantify sensitivity to initial conditions in dynamical systems, with positive exponents indicating chaos and limited predictability (Eckmann & Ruelle, 1985). These methods assume deterministic dynamics and require long, high-quality series for reliable estimation.

Practical and empirical approaches. Forecast Value Added (FVA) evaluates forecast performance relative to a simple baseline (Gilliland, 2010). If sophisticated methods cannot beat simple baselines, the series has low forecastability or the methods are poorly specified. FVA has proven valuable in operational contexts for identifying which forecasting activities add value, but it requires actual forecasting attempts and cannot be computed ex-ante from historical data alone.

Limitations of existing approaches. Three practical limitations constrain existing approaches in operational settings. First, horizon-dependence is ignored. Nearly all existing metrics produce single-valued scores (CV , ApEn, SampEn, spectral entropy, Lyapunov exponents). A series highly predictable at 1-step ahead may be unpredictable at 12-steps ahead, or vice versa. The relationship between short-term and long-term forecastability is complex and horizon-specific assessment is essential (Tiao & Tsay, 1994). Second, explicit alignment with forecast horizons is absent. Spectral

entropy summarises frequency-domain concentration but does not map directly to h -step-ahead prediction difficulty. Sample entropy provides a global regularity measure but does not specify which horizons benefit from that regularity. Lyapunov exponents indicate long-term predictability horizons in chaotic systems but not specific h -step-ahead difficulty. Third, comprehensive empirical validation is limited. Sample entropy showed promise in initial M3 studies (Catt, 2014) but comprehensive validation across diverse frequencies, horizons, and methods was not performed. Lyapunov exponents require long, well-resolved series to be estimated reliably and tend to perform poorly on the short, sparse series common in business forecasting settings (Wang, Klee, & Roos, 2025). CV continues to be used despite weak theoretical justification and inconsistent empirical support.

Our approach. We address these limitations through horizon-specific auto-mutual information (AMI). Spectral entropy measures overall frequency-domain concentration, but AMI at lag τ directly quantifies dependence between present values and values τ -steps in the past. Unlike entropy or spectral measures, AMI is explicitly indexed to forecast horizon, which is the key object of decision relevance. Sample entropy requires parameter selection, whereas AMI has a well-established non-parametric estimation framework via k -nearest neighbours. ACF captures only linear dependencies, but AMI captures both linear and nonlinear dependencies through its information-theoretic foundation. The key advantage of our framework is explicit lag-horizon mapping: AMI(τ) aligns to τ -step-ahead forecast difficulty. We compute AMI at lags corresponding to each forecast horizon h , making the connection between measurement and prediction operationally transparent. We then validate this framework comprehensively across M4 series, six frequencies, multiple horizons, and three forecasting methods, providing the empirical grounding that previous entropy-based approaches lacked.

2.3 Information-Theoretic Framework

Shannon (1948) defined entropy to quantify uncertainty in random variables:

$$H(X) = -\sum p(x) \log p(x)$$

For time series prediction, the relevant quantity is not marginal entropy $H(\text{Future})$ but conditional entropy $H(\text{Future} | \text{Past})$. The difference is mutual information:

$$I(\text{Past}; \text{Future}) = H(\text{Future}) - H(\text{Future} | \text{Past})$$

This quantity captures the reduction in uncertainty about the future attributable to the past.

For operational implementation, we use auto-mutual information (AMI), which quantifies shared information between a time series and its lagged self. At lag τ :

$$\text{AMI}(\tau) = I(X_t; X_{t+\tau}) = H(X_{t+\tau}) - H(X_{t+\tau} | X_t)$$

This is the mutual information between past and future. It measures how much the past tells you about the future. High predictive information means there's signal available to exploit. Entropy and mutual information are not redundant concepts. Two processes can have the same entropy rate but different 'organised structure'. AMI is the information-theoretic generalisation of the autocorrelation function, capturing both linear and nonlinear temporal dependencies (Fraser & Swinney, 1986; Kantz & Schreiber, 2004).

Bialek et al. (2001) formalised this as predictive information. Related constructs in computational mechanics include excess entropy and statistical complexity (Grassberger, 1986; Crutchfield & Feldman, 2003). The framework has deep precedent in physics, neuroscience, and computational theory where prediction and information processing are fundamental concerns (Palmer, 1999).

2.3.1 Forecastability, Exploitability, and Validation

A key distinction must be made between forecastability as dependence and forecastability as exploitability. AMI measures statistical dependence between past and future, a property of the data-generating process that exists independently of any forecasting method. However, whether that dependence translates into reduced forecast error depends on whether the forecasting method can represent and exploit the relevant structure.

AMI is therefore a diagnostic for available dependence, not a guarantee of error reduction under any particular loss function or hypothesis class. We validate AMI against realised sMAPE using Seasonal Naïve, ETS, and N-BEATS as probes of exploitability across different model classes. Where AMI correlates negatively with sMAPE, the dependence is being exploited. Where correlation is weak or absent, the mismatch is itself informative: it may indicate representation limitations (the model cannot capture the dependence structure), nonstationarity (in-sample dependence does not persist out-of-sample), or insufficient sample size (the dependence cannot be reliably estimated or learned).

3. Experimental Protocol

Figure 1 provides a conceptual intuition of the rolling-origin evaluation and the separation between pre-origin diagnostics (AMI) and post-origin outcomes (sMAPE). Panel A shows an expanding-window rolling-origin evaluation with multiple forecast origins. Panel B illustrates horizon-specific $AMI(h)$ computed pre-origin from the training data available at each origin. Panel C shows sMAPE evaluated post-origin for three probe models. Panel D demonstrates the key relationship: higher AMI corresponds to lower forecast error.

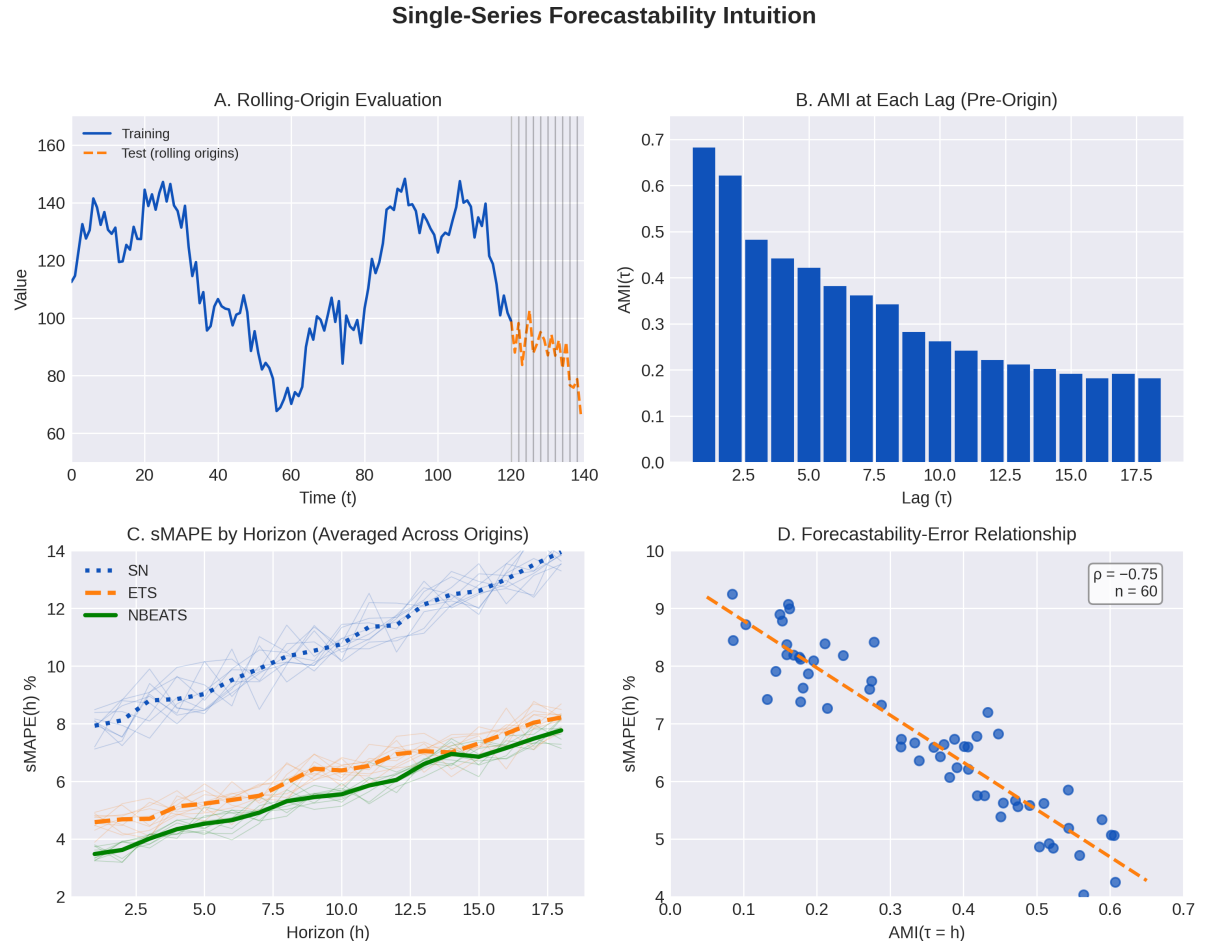


Figure 1. Conceptual forecastability intuition. (A) Expanding-window rolling-origin evaluation with 10 origins. (B) Horizon-specific $AMI(h)$ computed on training data available at each origin. (C) sMAPE evaluated post-

origin for each horizon and then averaged across origins. (D) Conceptual relationship tested empirically in Section 5: higher $AMI(h)$ is associated with lower realised $sMAPE(h)$ across series within frequency.

Figure 2 provides an illustrative view of how horizon-specific auto-mutual information (AMI) behaves under different forms of temporal structure. The examples are included solely to aid interpretation and are not used for model fitting, evaluation, or comparison.

Each row corresponds to a canonical process, with the left panel showing a representative standardised segment of the series for visual context and the right panel showing AMI estimated at increasing horizons on fixed illustrative windows. The processes span deterministic periodic behaviour (sine wave), real seasonal data with noise and trend (AirPassengers), low-dimensional chaotic dynamics (Hénon map), and weakly dependent stochastic behaviour (simulated stock returns).

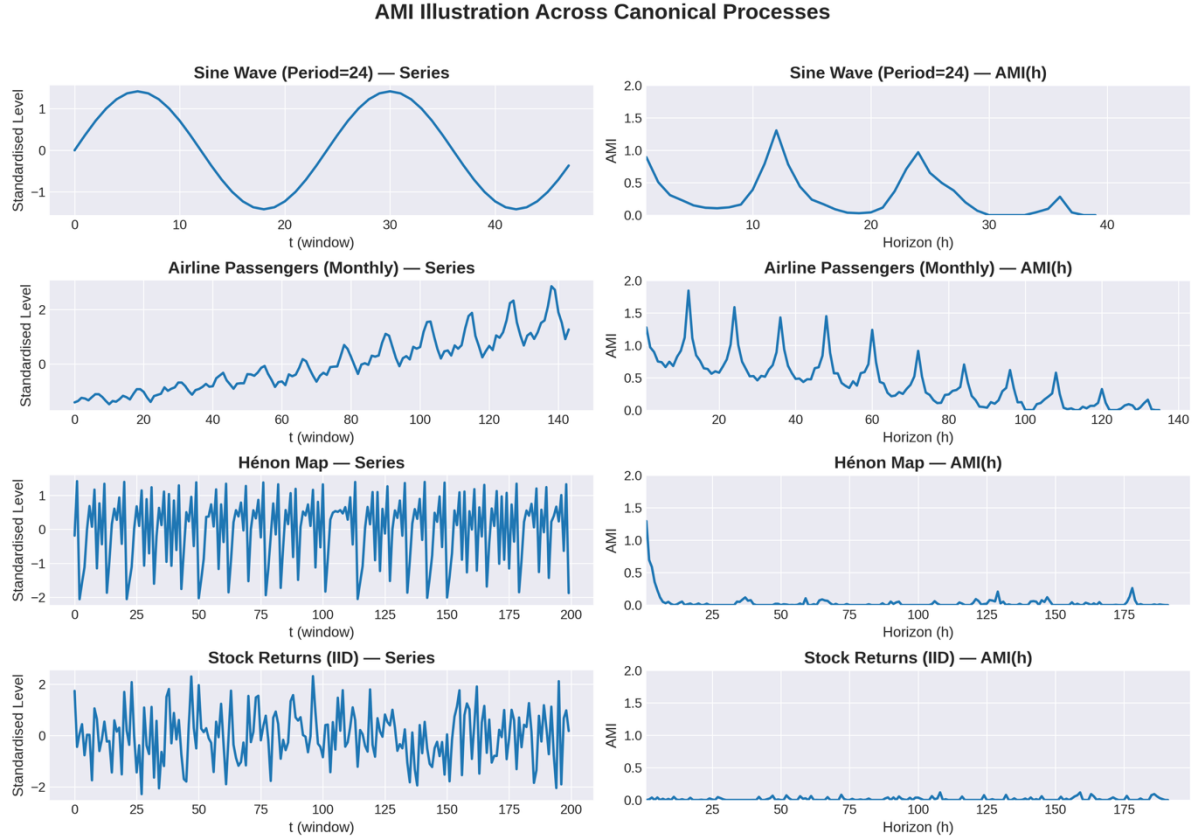


Figure 2. AMI illustration across canonical processes (interpretive only). Each row shows a representative standardised series segment (left) and its horizon-specific AMI profile (right), estimated using the same k NN MI estimator ($k = 8$) as the empirical study. These examples are for intuition only and are not used in model fitting, evaluation, or comparison.

To make the experimental protocol explicit and to separate pre-modelling diagnostics from post-origin evaluation, we describe the complete forecastability assessment pipeline. Three design choices merit emphasis. First, the protocol iterates over all horizons $h \in H$, computing a separate mutual information estimate at each lag; this traces the decay of past–future dependence as forecast distance increases. Second, AMI estimation uses a k -nearest-neighbour mutual information estimator, which provides consistent estimates for continuous variables without requiring density estimation or binning, a critical advantage over standard Shannon entropy approaches that struggle with real-valued time series. Third, the protocol enforces a strict rolling-origin constraint: each series is evaluated over 10 rolling forecast origins (no single-origin fallback). Local models (Seasonal Naïve, ETS) are re-fitted at each origin on information available at that origin. The global model (N-BEATS) is trained per frequency on pooled historical data and then used to generate roll-specific forecasts using only the history available at each origin (no future leakage). This preserves the ex-ante role of AMI (computed pre-origin from training data only) while reducing evaluation variance by averaging error across

origins. The protocol is intentionally asymmetric: diagnostics are computed strictly pre-origin using training data only and evaluated strictly post-origin against rolling held-out windows, preventing any leakage from outcomes into forecastability assessment.

This section describes the complete experimental methodology in sufficient detail for independent replication. All implementations use Python. We define all model specifications, survivorship rules, evaluation procedures, and forecastability computations. All reported results correspond to run_id = 20260119_151358.

3.1 M4 Dataset Overview

The M4 competition (Makridakis et al., 2020) provides 100,000 time series across six sampling frequencies: Yearly (23,000 series), Quarterly (24,000), Monthly (48,000), Weekly (359), Daily (4,227), and Hourly (414). Series span diverse domains including finance, industry, demographics, and macroeconomics. Each M4 series is provided with a training segment and a held-out test segment. In this study, forecasts are evaluated using a rolling-origin protocol constructed from the available historical data for each series (Section 3.3). The M4 test lengths are used only to define the maximum horizon H_{\max} by frequency (Hourly 48, Daily 14, Weekly 13, Monthly 18, Quarterly 8, Yearly 6), not to enforce use of the original M4 test split.

3.2 Survivor Panel Construction

From the full M4 dataset, we construct survivor panels for each frequency. The target sample sizes are: Hourly (100), Daily (200), Weekly (150), Monthly (300), Quarterly (300), and Yearly (300). These targets balance computational feasibility with statistical power for horizon-specific correlation analysis.

Survivor selection applies two sequential filters.

First, rolling-window feasibility: series must have sufficient history to support 10 rolling origins, each followed by a full H -step evaluation window. This ensures every survivor is evaluated at every required horizon under the rolling protocol (Section 3.3). Series that cannot support 10 full-origin evaluations are excluded.

Second, AMI feasibility: auto-mutual information must be computable at all required lags without numerical failure. Series where kNN estimation fails (typically due to degenerate distributions or insufficient effective sample size) are excluded.

From qualifying series, random stratified sampling by M4 category (Demographic, Finance, Industry, Macro, Micro, Other) is applied where category counts permit. When category counts are insufficient for balanced sampling, available series are included and remaining quota is filled from other categories.

Categories are used for balanced sampling and for checking robustness of the AMI–error relationship across semantic domains; the study is not designed to estimate causal or structural category effects, and we do not claim that categories drive forecastability.

Selection bias acknowledgement. Survivor panels represent the subset of series where AMI and sMAPE are numerically meaningful; results should not be interpreted as population averages over all M4 series. The feasibility filters necessarily exclude degenerate, extremely short, or numerically unstable series. This is appropriate for a diagnostic tool, since forecastability assessment is only meaningful where both the diagnostic and the forecast error metric can be reliably computed. Readers should note that the most problematic series (intermittent demand, near-constant, extremely short) are excluded by design. This is intentional: a diagnostic that cannot be computed reliably on a series cannot support pre-modelling decisions for that series; feasibility is part of operational applicability, not a limitation.

3.3 Forecast Origin and Horizon Structure

Forecasts are generated using an expanding-window rolling-origin design with exactly 10 origins per series (no single-origin fallback). For each frequency we define a horizon set $H = \{1, \dots, H_{\max}\}$, where H_{\max} is the frequency-specific maximum horizon. For each series we place 10 origins in the final portion of the usable history such that, at every origin, at least H_{\max} future observations exist for evaluation. At origin 0, models are estimated using only data up to 0 and are evaluated on the subsequent H_{\max} -step window. Forecast error is computed separately for each horizon h , and then averaged across the 10 origins for that horizon, yielding a per-horizon error profile with reduced variance relative to single-origin evaluation while maintaining strict pre-/post-origin separation.

3.4 Seasonal Naïve Baseline

Seasonal Naïve (SN) repeats the observation from the same seasonal position one cycle earlier. Formally:

$$\hat{y}_{t+h|t} = y_{t+h-km} \quad \text{where } k = \lceil h/m \rceil$$

This repeats the corresponding seasonal value from the most recent complete cycle, where m is the seasonal period (12 for Monthly, 4 for Quarterly, 52 for Weekly, 7 for Daily, 24 for Hourly). For Yearly data where no seasonal cycle exists, the last observed value is repeated (equivalent to Naïve).

Seasonal Naïve serves as a benchmark representing minimal modelling effort.

3.5 ETS Specification

ETS forecasts are generated using the exponential smoothing state space framework, with automatic selection over additive and damped trend components and additive or multiplicative seasonality where admissible, using information criteria for model choice. The implementation uses `statsmodels.tsa.holtwinters.ExponentialSmoothing` (Seabold & Perktold, 2010).

Multiplicative seasonality is permitted only when all observations are strictly positive. Box-Cox transformation is disabled to maintain interpretability and avoid numerical instability on diverse series.

The seasonal period is set to the M4-specified value for each frequency (12 for Monthly, 4 for Quarterly, 52 for Weekly, 7 for Daily, 24 for Hourly). For Yearly data where no seasonal cycle exists, the model reduces to non-seasonal exponential smoothing with trend selection. We use fixed seasonal periods for comparability across series; unlike M4's Naïve 2 benchmark, we do not conditionally test for seasonality.

Point forecasts are generated for all horizons $h = 1, \dots, H_{\max}$ from the selected model.

3.6 N-BEATS Specification

N-BEATS (Neural Basis Expansion Analysis for Time Series; Oreshkin et al., 2020) is implemented using the `neuralforecast` library (Olivares et al., 2022). A single global model is trained per frequency on a pooled panel of series and then applied to generate forecasts for all survivor series in that frequency. The trained global model is applied under rolling-origin evaluation (10 origins per series), with no use of future information beyond each origin.

Training uses MAE loss with generic stacks; early stopping is disabled to ensure full convergence. A synthetic daily timeline is used for all frequencies to prevent datetime overflow with high-frequency data. The key property for our purposes is that N-BEATS represents a fundamentally different model class from ETS (global, nonlinear, and neural), enabling tests of whether AMI-sMAPE relationships are robust across architectures.

3.7 Forecast Error Metric: sMAPE

Symmetric Mean Absolute Percentage Error (sMAPE) is used throughout. For a single series at horizon h :

$$\text{sMAPE}(h) = \frac{2|y_{t+h} - \hat{y}_{t+h|t}|}{|y_{t+h}| + |\hat{y}_{t+h|t}|}$$

sMAPE is bounded between 0 and 2 (or 0% to 200%), scale-independent, and symmetric in over- and under-prediction. It avoids the instability that can arise in MASE when the scaling denominator is very small or undefined for short or near-constant series. (Hyndman & Koehler, 2006). We report sMAPE as a percentage (i.e., $\text{sMAPE} \times 100$) in all tables and figures. Accordingly, all reported sMAPE values are on a 0–200 scale.

3.8 AMI Computation

Auto-mutual information (AMI) is computed using a k-nearest-neighbour mutual information estimator implemented via `mutual_info_regression` (scikit-learn). This class of estimators provides consistent mutual information estimates without requiring explicit density estimation or discretisation, though it exhibits finite-sample bias that decreases with sample size (Kraskov et al., 2004). All statistical inference in this study relies on rank association (Spearman ρ), which mitigates sensitivity to monotone estimator bias; conclusions depend on AMI correctly ranking series by forecastability rather than on absolute MI magnitudes.

Under the rolling-origin evaluation protocol, AMI is recomputed separately for each roll using the training data available up to that origin. For each roll and each forecast horizon $h = 1, \dots, H_{\max}$, $\text{AMI}(h)$ is estimated as the mutual information $I(y_t; y_{t+h})$, using all valid indices t such that both observations lie strictly within the roll-specific training window. Under no circumstances are post-origin observations used in AMI estimation.

The kNN parameter is fixed globally at $k = 8$ across all frequencies, horizons, and rolls for reproducibility. Series for which AMI estimation fails at any required horizon, typically due to degenerate distributions or insufficient effective sample size, are excluded during survivor selection prior to forecasting.

Interpretation note. The AMI values reported here are relative measures used for ranking and triage, not absolute information quantities in nats or bits. Short-series bias is mitigated via minimum effective sample size requirements in survivor filtering; remaining estimator bias is addressed by relying on Spearman rank correlations and frequency-conditional analysis rather than absolute AMI magnitudes.

Reproducibility. All reported results correspond to a single fully deterministic rolling-origin run. While multiple forecast origins are evaluated per series, all survivor selection, AMI computation, model estimation, and error aggregation are executed with fixed random seeds and predefined specifications. No hyperparameter tuning or post-hoc model selection is performed. For reporting and correlation analysis, $\text{AMI}(h)$ and $\text{sMAPE}(h)$ are averaged across the 10 rolling origins for each series. Given the M4 dataset and the documented protocol, all results are exactly reproducible. All reported results correspond to `run_id = 20260119_151358`, as recorded in the run outputs and associated manifest.

4. Data Description

4.1 M4 Dataset Structure and Survivor Selection

The M4 competition dataset contains 100,000 time series across six frequencies. Table 1 summarises the dataset structure and survivor selection outcomes.

Table 1: Dataset Composition and Survivor Selection

Frequency	Total M4	Eligible (approx.)	Target	Selected
Hourly	414	~380	100	100
Daily	4,227	~3,950	200	200
Weekly	359	~340	150	150
Monthly	48,000	~42,000	300	300
Quarterly	24,000	~21,000	300	300
Yearly	23,000	~18,000	300	300

Notes: Eligible counts are approximate, computed after length filters.

The binding constraint varies by frequency. For Weekly, the small M4 pool (359 series) limits available survivors. For Monthly and Quarterly, AMI feasibility is the primary filter. Yearly requires evaluation of approximately 1,010 series to obtain 300 survivors, with AMI infeasibility as the main exclusion mechanism.

5. Results

This section reports empirical findings from the experimental protocol described in Section 3. We present sample coverage, the relationship between forecastability measures (AMI) and realised forecast error (sMAPE), robustness analysis by training length, and decision utility of AMI-based triage.

5.1 Sample Coverage

The survivor panels achieved their targets: Hourly ($n = 100$), Daily ($n = 200$), Weekly ($n = 150$), Monthly ($n = 300$), Quarterly ($n = 300$), and Yearly ($n = 300$). Total survivors across frequencies is 1,350 series. All three models (Seasonal Naïve, ETS, and N-BEATS) produced forecasts at all horizons for the survivor series included in the reported analyses.

5.2 Probe Model Context

Before examining the core AMI-sMAPE relationship, we briefly characterise the probe models to establish that they span different representational capacities and that subsequent results are not artefacts of a particular forecasting architecture. Probe models are used to test whether forecastability rankings persist across model capacity, not to compete for best accuracy; relative probe performance is incidental to the diagnostic question.

Probe models differ in absolute accuracy by frequency; these differences are incidental to the diagnostic objective. N-BEATS achieves lowest median sMAPE at high frequencies (Hourly, Daily, Weekly), while ETS is competitive at lower frequencies (Quarterly, Yearly). Seasonal Naïve serves as a minimal-complexity baseline throughout. Daily can still have low median error while exhibiting weak cross-series discrimination by AMI.

Across all frequencies, forecast error increases monotonically with horizon (Figure 3), confirming that horizon itself drives forecast difficulty.

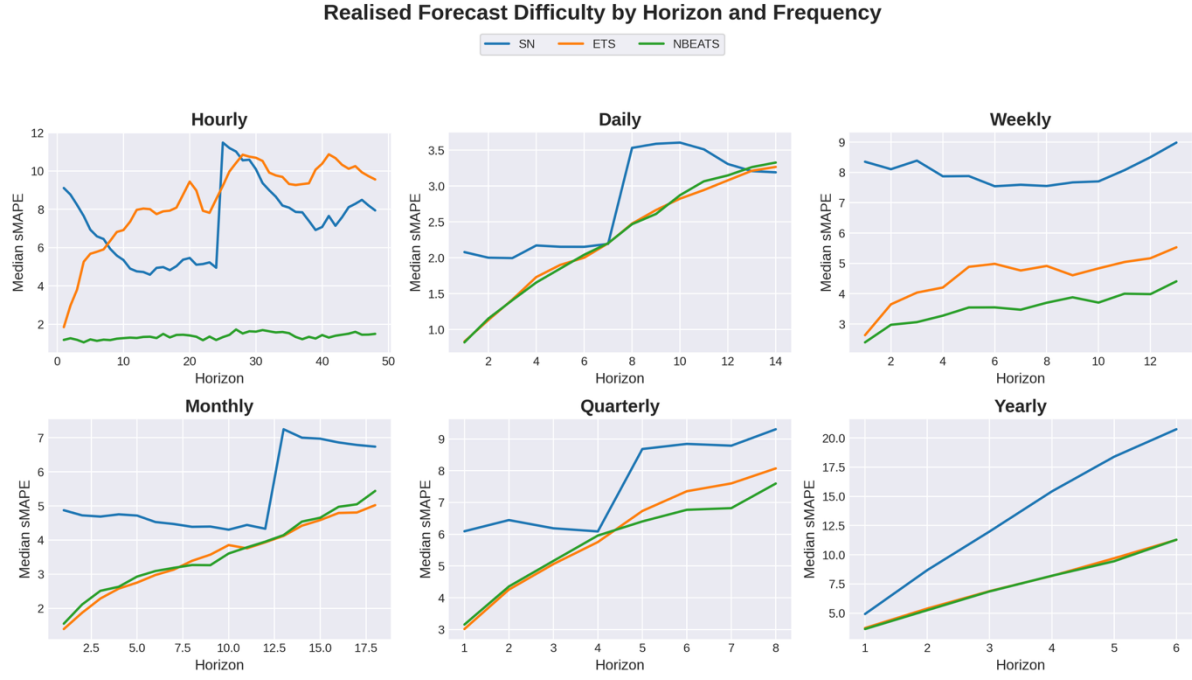


Figure 3. *Realised forecast difficulty by horizon and frequency. Each panel shows median sMAPE across survivor series, where each series' sMAPE(h) is first averaged across the 10 rolling origins. Median error generally increases with horizon, with occasional local non-monotonicity. Horizon ranges are frequency-specific (Hourly 1–48, Daily 1–14, Weekly 1–13, Monthly 1–18, Quarterly 1–8, Yearly 1–6).*

5.3 Forecastability Measures and Realised Error

A clarification is essential before presenting results. We do not estimate which frequency is harder overall (absolute difficulty); we estimate whether AMI ranks series within a frequency by forecast difficulty at that frequency's horizons (cross-series discrimination). The contribution is within-frequency triage, not between-frequency difficulty rankings.

Figure 4 illustrates the decay of forecastability (AMI) with horizon. Auto-mutual information profiles computed on training data exhibit systematic decay with lag across all frequencies, consistent with diminishing past–future dependence as forecast distance increases. Lag axes reflect frequency-specific horizon ranges. This decay confirms that forecastability is inherently horizon-specific, reinforcing the need for horizon-aligned diagnostics.

Horizon Profile of Training-Only AMI by Frequency

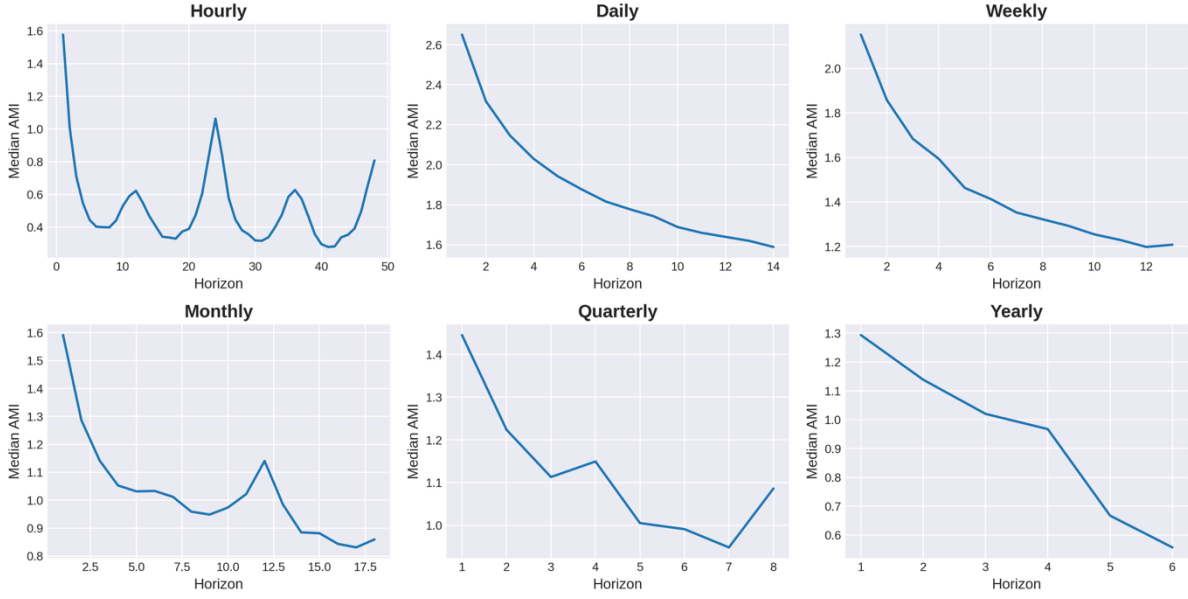


Figure 4. AMI decay with horizon. Profiles show the median $AMI(h)$ across survivor series, after averaging $AMI(h)$ across rolling origins per series. Auto-mutual information profiles computed on training data exhibit systematic decay with lag across all frequencies, consistent with diminishing past–future dependence as forecast distance increases. Lag axes reflect frequency-specific horizon ranges.

The AMI–sMAPE relationship varies systematically by frequency, with strong negative associations at some frequencies and materially weaker associations at others. We assess whether AMI behaves as an operational measure of forecastability by examining Spearman rank correlations between AMI and sMAPE. Consistent with the interpretation of AMI as an ordinal diagnostic, we report rank association rather than linear fit: the objective is stable ordering of series by expected difficulty within each frequency, not prediction of absolute error levels.

Table 2: Forecastability–Accuracy Relationship (AMI Validation)

Frequency	Seasonal Naïve	ETS	N-BEATS
Hourly	-0.46	-0.29	-0.52
Daily	-0.16	-0.14	-0.14
Weekly	-0.22	-0.66	-0.66
Monthly	-0.17	-0.34	-0.33
Quarterly	-0.45	-0.55	-0.58
Yearly	-0.20	-0.55	-0.60

Notes: Spearman rank correlation computed per horizon across survivor series, then averaged across horizons within each (frequency, model).

Table 2 reports the primary validation: Spearman rank correlations computed per horizon across survivor series, then averaged across horizons within each (frequency, model). Under this protocol, Hourly, Weekly, Quarterly, and Yearly series show strong negative rank association between training-only AMI and realised out-of-sample sMAPE across all probe models. Weekly exhibits the strongest relationships for the higher-capacity probes (ETS $\rho = -0.66$, N-BEATS $\rho = -0.66$), consistent with AMI identifying dependence that is exploitable by both classical state-space structure and global

nonlinear architectures. Hourly also shows substantial association (N-BEATS $\rho = -0.52$), and the relationship remains strong at Quarterly (N-BEATS $\rho = -0.58$) and Yearly (N-BEATS $\rho = -0.60$). Monthly exhibits moderate negative association for ETS ($\rho = -0.34$) and N-BEATS ($\rho = -0.33$), and weaker association for Seasonal Naïve ($\rho = -0.17$), consistent with dependence that simple seasonal repetition fails to exploit.

Daily is an empirical weak-discrimination case under this protocol. Although AMI indicates non-trivial past–future dependence within daily series, its rank association with realised sMAPE is materially weaker than for other frequencies (approximately $\rho = -0.14$ to -0.16 across probes). This indicates reduced cross-series discriminative power for triage: variation in AMI corresponds to comparatively smaller variation in realised error within the daily survivor panel. This does not imply absence of dependence, but it does limit the usefulness of AMI as a within-frequency screening signal for Daily in the present setting.

As a robustness check, we confirmed that the qualitative conclusions in Table 2 are unchanged under alternative aggregation choices, including pooling horizons within frequency to compute a single Spearman correlation and reporting the median rather than the mean of horizon-specific correlations. These alternatives change magnitudes (as expected) but do not induce sign reversals or frequency-level reordering, indicating that the results reflect stable within-frequency rank association rather than artefacts of a specific summarisation.

Figure 5 presents a heatmap showing the Spearman correlation between AMI and sMAPE by frequency and horizon. Blue cells indicate negative correlation (higher AMI associated with lower error), confirming that AMI serves as a consistent forecastability indicator for most frequencies, with Daily exhibiting weak and non-monotone association. The contribution lies in ordinal separation for triage, not linear predictability.

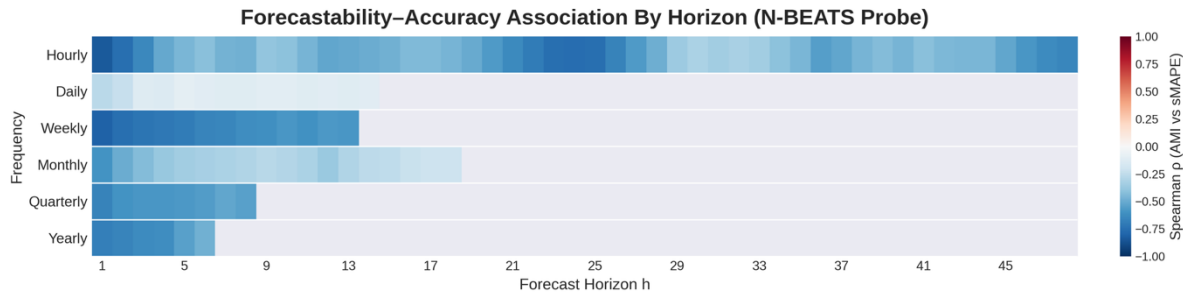


Figure 5. Forecastability-Accuracy Association by Frequency and Horizon (N-BEATS). Spearman correlation (ρ) between AMI and sMAPE by frequency and horizon (N-BEATS probe). Each cell shows series-level Spearman ρ computed across all survivor series within each (frequency, horizon) combination; blue indicates negative correlation (higher AMI associated with lower error). Cells are shown only for horizons defined for each frequency (Hourly 1–48, Daily 1–14, Weekly 1–13, Monthly 1–18, Quarterly 1–8, Yearly 1–6); blank regions are not missing data.

Role of categories relative to frequency. Series categories are incorporated primarily to ensure balanced sampling and to check robustness against dominance by any single domain. To assess whether semantic domain materially alters the relationship between dependence and forecast difficulty, we examined the direction of the AMI–sMAPE association within categories for each frequency. Across frequencies, we do not observe systematic category-level sign reversals relative to the corresponding frequency-level pattern. While association strength varies across categories and statistical power is limited in some cells (notably for Weekly series), the direction of association is broadly consistent. Accordingly, category is treated as a secondary conditioning dimension: forecastability is shaped primarily by temporal resolution and forecast horizon, with semantic domain playing a supporting rather than dominant role.

5.4 Robustness: Training Length Effects

A natural concern is whether AMI–sMAPE correlations are confounded by series length. Stratified analysis within each frequency shows that negative correlations persist across all training-length terciles (Table 3), indicating that the forecastability signal is not merely a proxy for series length. We report tercile stratification for the global probe (N-BEATS) as an illustrative check; results are qualitatively similar for ETS.

Table 3: AMI–sMAPE Correlations by Training Length Tercile (N-BEATS)

Frequency	Short	Medium	Long
Weekly	−0.44	−0.75	−0.84
Monthly	−0.38	−0.24	−0.45
Yearly	−0.63	−0.59	−0.56

Notes: Series are stratified into terciles by training length within each frequency. Values are Spearman ρ between AMI and sMAPE within each tercile. N-BEATS reported as an illustrative global probe; ETS shows qualitatively similar patterns.

5.5 Decision Utility of Forecastability Assessment

The practical value of forecastability assessment lies in its ability to inform resource allocation decisions before forecasting begins. Table 4 demonstrates this by showing median sMAPE conditional on AMI terciles.

Table 4: Decision Utility — Median sMAPE by AMI Tercile

Frequency	SN Low	SN Mid	SN High	ETS Low	ETS Mid	ETS High	NB Low	NB Mid	NB High
Hourly	10.65	13.21	1.66	11.22	16.13	0.68	2.88	6.50	0.48
Daily	3.08	2.42	2.13	2.44	2.01	1.54	2.49	2.03	1.54
Weekly	10.79	8.13	6.51	9.68	4.68	1.60	8.02	3.59	1.43
Monthly	6.88	4.92	4.13	5.19	3.36	1.91	5.44	3.39	2.17
Quarterly	13.08	7.98	4.67	11.21	6.82	2.59	11.42	6.44	2.58
Yearly	15.10	9.77	8.76	14.09	7.50	3.34	14.87	7.65	3.00

Notes: AMI terciles computed within each frequency across all valid (series, horizon) pairs. Values are median sMAPE (%).

Across all six frequencies, median sMAPE decreases monotonically from Low to High AMI terciles for each probe model (Table 4), confirming that AMI supports decision-relevant ordinal separation even when rank correlations are weaker. The discrimination is steepest for Hourly and Weekly: for ETS, median sMAPE falls by approximately 94% from Low to High AMI terciles at Hourly (11.22 to 0.68) and by approximately 83% at Weekly (9.68 to 1.60); N-BEATS shows similarly strong separation (Hourly 2.88 to 0.48; Weekly 8.02 to 1.43). These gradients indicate that AMI-based triage can function as an operational screening layer: high-AMI series justify investment in model development and monitoring, while low-AMI series are better served by baselines and by shifting effort towards consequence mitigation and robust decision design.

6. Discussion

These results support a simple conceptual point: forecastability is not a single scalar property of a series, but a horizon-specific relationship between past and future under a declared information set. Forecast models operate within these informational constraints; they do not create predictive information where the series contains little usable past–future dependence at the decision horizon.

6.1 The AMI–Error Relationship is Frequency-Conditional

The dominant finding of this study is that the AMI–sMAPE relationship is strongly frequency-conditional. At Hourly, Weekly, Quarterly, and Yearly frequencies, AMI computed from training data provides a valid diagnostic signal for out-of-sample forecast difficulty across all probe models. Monthly frequency exhibits an intermediate pattern where signal emerges only with sophisticated methods. For Daily series, AMI indicates non-trivial past–future dependence, but its rank association with realised sMAPE is materially weaker than for other frequencies under the present protocol, implying reduced discriminative power for within-frequency triage.

This finding establishes an operational constraint for AMI-based triage: the diagnostic should be validated within each application context rather than assumed universal. These observed associations are empirical and protocol-specific rather than universal laws of predictability.

6.2 Daily frequency: dependence present, weaker discriminative power

Daily series show substantial past–future dependence (AMI) in absolute terms, yet forecast error is low in absolute terms across the probe models. Consistent with this compression of error, the AMI–sMAPE association is weaker for Daily than for most other frequencies: variation in AMI provides limited discrimination among already accurate series, even though dependence itself is clearly present. This should be read as a frequency-conditional limitation on the triage value of AMI for Daily under the present rolling-origin evaluation protocol, not as evidence that temporal dependence is absent.

6.3 Forecastability versus Exploitability

A conceptual distinction is necessary. *Forecastability* as we define it, namely AMI between past and future, is a property of the series itself, independent of any forecasting model. It measures statistical dependence in the data-generating process. *Exploitability* is the degree to which a particular model class can convert that dependence into accurate forecasts.

AMI measures total dependence; the fraction that translates to error reduction depends on the model’s hypothesis class. At Weekly frequency, all probes exhibit strong negative association between AMI and sMAPE, with ETS and N-BEATS strongest (both $\rho = -0.66$) and Seasonal Naïve weaker ($\rho = -0.22$). This pattern, where different probe models exhibit varying association strengths against the same underlying dependence, supports the distinction between forecastability (available dependence) and exploitability (model capacity to convert that dependence into accuracy under the chosen loss and protocol).

6.4 Moderating Factors

Beyond frequency and horizon, several factors moderate the forecastability-accuracy relationship. Series length affects both AMI estimation variance and the training signal available to statistical and neural models; shorter series yield noisier diagnostics and less reliable forecasts regardless of method. Seasonal strength matters because stable, repeating patterns benefit structured models like ETS and even Seasonal Naïve, whereas weak or evolving seasonality favours more flexible approaches. Variance structure and scale effects may also influence the AMI-sMAPE relationship, though this study did not directly test these dimensions.

Structural breaks and regime instability present a more fundamental challenge, as they can sever the link between in-sample dependence and out-of-sample difficulty. Since we treat the data-generating process as latent and measure only its observable consequence (past-future dependence in the realised training segment), forecastability diagnostics are inherently conditional on the assumption that the future segment is governed by a similar process. When regimes shift, historical dependence patterns may not persist. Finally, cross-series heterogeneity affects global models: pooled learning benefits portfolios with shared structure but offers diminishing returns when series are fundamentally dissimilar.

This study explicitly tested frequency, horizon, and series length effects. Seasonal strength, variance structure, and regime stability remain avenues for future investigation.

6.5 Implications for Multivariate Forecasting

Although the empirical analysis focuses on univariate series, the findings carry direct implications for multivariate forecasting contexts. The use of global models introduces a form of implicit multivariate learning by exploiting shared structure across a large panel of series, without requiring explicit specification of cross-series dependencies. Our results suggest that forecastability is primarily governed by temporal resolution and effective information content within individual series, which implies that univariate forecastability is a necessary, though not sufficient, condition for value creation in multivariate models.

This leads to a practical gating rule: multivariate enrichment should be attempted only when univariate forecastability is low but plausible external drivers exist at the decision horizon. If univariate AMI is already high, covariates are unlikely to add value because the target series already contains sufficient predictive structure. Conversely, if univariate AMI is low and no leading indicators exist, covariates will not rescue an inherently unforecastable target. A related consideration is measurement cadence: low-frequency series are unlikely to benefit from covariates unless those covariates are measured at higher cadence and genuinely lead the target. Annual series paired with annual covariates simply compound information scarcity.

6.6 Implications for Decision Workflows

These findings support a concrete pre-modelling diagnostic workflow. Before committing forecasting resources, practitioners should first identify the temporal resolution and decision-relevant horizon, since frequency determines baseline expectations for forecastability. The AMI-sMAPE relationship is strongest for Weekly and remains substantial for Hourly and Quarterly. Next, AMI should be computed at relevant lags, noting training series length as a moderating factor.

Based on frequency, AMI level, and series characteristics, each series can then be assigned to an appropriate modelling regime. Series with high AMI at Weekly or Hourly frequency warrant investment in more sophisticated models such as ETS or global neural architectures, where the strong negative AMI-sMAPE correlations (Table 2) indicate meaningful accuracy gains over simple baselines. Series in the middle AMI tercile, or at Monthly and Quarterly frequencies, merit standard models with managed horizon expectations; ensemble or robustified approaches may be appropriate. Series with low AMI or unstable AMI estimation are better served by simple baselines. For these series, resources should shift from forecast refinement toward consequence mitigation: safety stock sizing, scenario planning, cadence adjustment, or decision architectures that are robust to forecast error.

This workflow operationalises the core finding: forecastability assessment should precede model selection, and the appropriate action depends on both frequency and measured dependence strength.

6.7 Limitations and Future Research

Several limitations warrant acknowledgement. Survivorship filtering was necessary to compute AMI reliably, which means that forecastability assessment is only meaningful where it is definable. The

method is best framed as a ‘feasible where definable’ triage tool rather than a universal measure applicable to all series.

Validation used three specific forecasting methods on M4 data. While the conceptual framework is general, empirical relationships are context-dependent, and domain-specific validation remains essential before operational deployment. This study also focuses exclusively on point forecast accuracy measured via sMAPE; probabilistic forecasting, density forecast evaluation, and decision-theoretic loss functions may exhibit different relationships with AMI.

Finally, horizon-specific forecastability is conditioned on the realised DGP segment observed in the training window. If the underlying data-generating process changes between estimation and forecast periods, in-sample dependence will not predict out-of-sample difficulty.

7. Conclusions and Recommendations

This study developed and validated an information-theoretic framework for assessing time series forecastability as horizon-specific past–future dependence. Using an expanding-window rolling-origin protocol with 10 origins per series and computing AMI strictly from training data, we evaluated whether AMI ranks series by realised out-of-sample error (sMAPE) within each frequency. The central finding is that the AMI–sMAPE relationship is strongly frequency-conditional under this protocol. For Hourly, Weekly, Quarterly, and Yearly (and to a moderate extent Monthly), AMI exhibits consistently negative rank association with sMAPE across probe models, with particularly strong effects at Weekly and substantial effects at Hourly, Quarterly, and Yearly. Daily exhibits materially weaker rank association under the same protocol, implying reduced discriminative power for within-frequency triage despite measurable dependence.

A conceptual distinction between forecastability and exploitability is useful for interpretation. AMI measures horizon-aligned dependence in the realised training segment, whereas exploitability reflects the extent to which a given model class can convert that dependence into reduced error under a specific evaluation protocol. Consistent with this, association magnitudes differ across probes, with ETS and N-BEATS generally showing stronger rank associations than Seasonal Naïve.

For practitioners, the findings support a decision workflow that places forecastability assessment before model selection. First stratify by frequency and decision-relevant horizon. Then compute horizon-specific AMI as an ordinal screening signal to rank series by expected difficulty within frequency. Where AMI is high, investment in more expressive modelling approaches is warranted; where AMI is low, returns to modelling effort diminish and attention should shift towards robust decision design (for example, safety stock, scenario planning, or policies that reduce sensitivity to forecast error). The contribution is not a new forecasting algorithm but a diagnostic layer that addresses a practitioner-critical question: not “which model is best?”, but “is this series worth modelling at all?” under the declared information set and decision horizon.

References

Bialek, W., Nemenman, I., & Tishby, N. (2001). Predictability, complexity, and learning. *Neural Computation*, 13(11), 2409–2463.

Catt, P. M. (2009). Forecastability: Insights from physics, graphical decomposition, and information theory. *Foresight: The International Journal of Applied Forecasting*, 13, 24–33.

Catt, P. M. (2014). Entropy as an a priori indicator of forecastability [Working paper]. ResearchGate.

Cover, T. M., & Thomas, J. A. (2006). *Elements of information theory* (2nd ed.). Wiley.

Crutchfield, J. P., & Feldman, D. P. (2003). Regularities unseen, randomness observed: Levels of entropy convergence. *Chaos*, 13(1), 25–54.

Delgado-Bonal, A., & Marshak, A. (2019). Approximate entropy and sample entropy: A comprehensive tutorial. *Entropy*, 21(6), 541.

Eckmann, J.-P., & Ruelle, D. (1985). Ergodic theory of chaos and strange attractors. *Reviews of Modern Physics*, 57(3), 617–656.

Fraser, A. M., & Swinney, H. L. (1986). Independent coordinates for strange attractors from mutual information. *Physical Review A*, 33(2), 1134–1140.

Gilliland, M. (2010). *The business forecasting deal*. Wiley.

Goerg, G. M. (2013). Forecastable component analysis. In *Proceedings of the 30th International Conference on Machine Learning* (pp. 64–72). PMLR.

Grassberger, P. (1986). Toward a quantitative theory of self-generated complexity. *International Journal of Theoretical Physics*, 25(9), 907–938.

Hyndman, R. J., & Koehler, A. B. (2006). Another look at measures of forecast accuracy. *International Journal of Forecasting*, 22(4), 679–688.

Jaynes, E. T. (1957). Information theory and statistical mechanics. *Physical Review*, 106(4), 620–630.

Kantz, H., & Schreiber, T. (2004). *Nonlinear time series analysis* (2nd ed.). Cambridge University Press.

Kolassa, S. (2009). Can we obtain valid benchmarks from published surveys of forecast accuracy? *Foresight: The International Journal of Applied Forecasting*, 14, 6–12.

Kraskov, A., Stögbauer, H., & Grassberger, P. (2004). Estimating mutual information. *Physical Review E*, 69(6), 066138.

Makridakis, S., & Hibon, M. (2000). The M3-competition: Results, conclusions and implications. *International Journal of Forecasting*, 16(4), 451–476.

Makridakis, S., Andersen, A., Carbone, R., Fildes, R., Hibon, M., Lewandowski, R., Newton, J., Parzen, E., & Winkler, R. (1982). The accuracy of extrapolation (time series) methods: Results of a forecasting competition. *Journal of Forecasting*, 1(2), 111–153.

Makridakis, S., Spiliotis, E., & Assimakopoulos, V. (2018). The M4 competition: Results, findings, conclusion and way forward. *International Journal of Forecasting*, 34(4), 802–808.

Makridakis, S., Spiliotis, E., & Assimakopoulos, V. (2020). The M4 competition: 100,000 time series and 61 forecasting methods. *International Journal of Forecasting*, 36(1), 54–74.

Olivares, K. G., Challu, C., Marcjasz, G., Weron, R., & Dubrawski, A. (2022). NeuralForecast: User-friendly state-of-the-art neural forecasting models. In *Proceedings of the 21st Python in Science Conference* (pp. 1–9). <https://github.com/Nixtla/neuralforecast>.

Oreshkin, B. N., Carpow, D., Chapados, N., & Bengio, Y. (2020). N-BEATS: Neural basis expansion analysis for interpretable time series forecasting. In *International Conference on Learning Representations*. <https://openreview.net/forum?id=r1ecqn4YwB>.

Palmer, S. E. (1999). *Vision science: Photons to phenomenology*. MIT Press.

Petropoulos, F., Apiletti, D., Assimakopoulos, V., Babai, M. Z., Barrow, D. K., Ben Taieb, S., Bergmeir, C., Bessa, R. J., Bijak, J., Boylan, J. E., Browell, J., Carnevale, C., Castle, J. L., Cirillo, P., Clements, M. P., Cordeiro, C., Cyrino Oliveira, F. L., De Baets, S., Dokumentov, A., ... Ziel, F. (2022). Forecasting: Theory and practice. *International Journal of Forecasting*, 38(3), 845–1154.

Pincus, S. M. (1991). Approximate entropy as a measure of system complexity. *Proceedings of the National Academy of Sciences*, 88(6), 2297–2301.

Richman, J. S., & Moorman, J. R. (2000). Physiological time-series analysis using approximate entropy and sample entropy. *American Journal of Physiology-Heart and Circulatory Physiology*, 278(6), H2039–H2049.

Seabold, S., & Perktold, J. (2010). Statsmodels: Econometric and statistical modeling with Python. In *Proceedings of the 9th Python in Science Conference* (pp. 57–61). SciPy.

Shannon, C. E. (1948). A mathematical theory of communication. *Bell System Technical Journal*, 27(3), 379–423.

Stock, J. H., & Watson, M. W. (2003). Forecasting output and inflation: The role of asset prices. *Journal of Economic Literature*, 41(3), 788–829.

Tiao, G. C., & Tsay, R. S. (1994). Some advances in non-linear and adaptive modelling in time-series. *Journal of Forecasting*, 13(2), 109–131.

Wang, R., Klee, S., & Roos, A. (2025). Time series forecastability measures. In *Proceedings of the 1st Workshop on "AI for Supply Chain: Today and Future" @ 31st ACM SIGKDD Conference on Knowledge Discovery and Data Mining (KDD '25)*. ACM.